Krishnamoorthy, G., & Hinkle, P. C. (1984) *Biochemistry 23*, 1640–1645.
LaNoue, K. F., & Schoolwerth, A. C. (1979) *Annu. Rev. Biochem. 48*, 871–922.
Maloney, P. C., & Hansen, F. C., III (1982) *J. Membr. Biol. 66*, 63–75.
Massari, S., Frigeri, L., & Azzone, G. F. (1972a) *J. Membr. Biol. 9*, 57–70.
Massari, S., Frigeri, L., & Azzone, G. F. (1972b) *J. Membr. Biol. 9*, 71–82.
Mitchell, P. D., & Moyle, J. (1967) *Biochem. J. 104*, 588–600.
Nicholls, D. G. (1974) *Eur. J. Biochem. 50*, 306–315.
Nicholls, D. G. (1977) *Eur. J. Biochem. 77*, 349–356.
O'Shea, P., Petrone, G., Casey, R. P., & Azzi, A. (1984) *Biochem. J. 219*, 719–726.
Pietrobon, D., Azzone, G. F., & Walz, D. (1981) *Eur. J. Biochem. 117*, 389–394.
Peitrobon, D., Zoratti, M., Azzone, G. F., Stucki, J. W., & Walz, D. (1982) *Eur. J. Biochem. 127*, 483–494.
Pietrobon, D., Zoratti, M., & Azzone, G. F. (1983) *Biochim. Biophys. Acta 723*, 317–321.
Pietrobon, D., Zoratti, M., Azzone, G. F., & Caplan, S. R. (1986) *Biochemistry* (following paper in this issue).
Rossi, E., & Azzone, G. F. (1969) *Eur. J. Biochem. 7*, 418–426.
Rottenberg, H., & Solomon, A. K. (1969) *Biochim. Biophys. Acta 193*, 48–57.
Schlodder, E., Graeber, P., & Witt, H. T. (1982) in *Electron Transport and Phosphorylation* (Barber, J., Ed.) pp 107–167, Elsevier Biomedical Press, Amsterdam.
Sorgato, M. C., & Ferguson, S. J. (1979) *Biochemistry 18*, 5737–5742.
Tedeschi, H., & Harris, D. L. (1955) *Arch. Biochem. Biophys. 58*, 52–67.
Tedeschi, H., & Harris, D. L. (1958) *Biochim. Biophys. Acta 28*, 392–402.
Zoratti, M., Favaron, M., Pietrobon, D., & Petronilli, V. (1984) *Biochim. Biophys. Acta 767*, 231–239.

Intrinsic Uncoupling of Mitochondrial Proton Pumps. 2. Modeling Studies†

Daniela Pietrobon,*,‡,§ Mario Zoratti,‡ Giovanni Felice Azzone,‡ and S. Roy Caplan§
Department of Membrane Research, The Weizmann Institute of Science, Rehovot 76100, Israel, and CNR Unit for the Study of the Physiology of Mitochondria, Institute of General Pathology, University of Padova, 35100 Padova, Italy
Received June 6, 1985

ABSTRACT: The thermodynamic and kinetic properties associated with intrinsic uncoupling in a six-state model of a redox proton pump have been studied by computing the flow–force relations for different degrees of coupling. Analysis of these relations shows the regulatory influence of the thermodynamic forces on the extent and relative contributions of redox slip and proton slip. Inhibition has been introduced into the model in two different ways, corresponding to possible modes of action of experimental inhibitors. Experiments relating the rate of electron transfer to $\Delta\tilde{\mu}_H$ at static head upon progressive inhibition of the pumps have been simulated considering (1) the limiting case that the nonzero rate of electron transfer at static head is only due to intrinsic uncoupling (no leaks) and (2) the experimentally observed case that about 30% of the nonzero rate of electron transfer at static head is due to a constant proton leakage conductance in parallel with the pumps, the rest being due to intrinsic uncoupling. The same simulations have been performed for experiments in which the rate of electron transfer is varied by varying the substrate concentration rather than by using an inhibitor. The corresponding experimental results obtained by measuring $\Delta\tilde{\mu}_H$ and the rate of electron transfer at different succinate concentrations in rat liver mitochondria are presented. Comparison between simulated behavior and experimental results leads to the general conclusion that the typical relationship between rate of electron transfer and $\Delta\tilde{\mu}_H$ found in mitochondria at static head could certainly be a manifestation of some degree of intrinsic uncoupling in the redox proton pumps. The physiological significance of this conclusion and its implications with regard to the interpretation of measurements of the stoichiometry of coupled processes are discussed.

An ion pump promotes the coupling between a scalar reaction and a transmembrane vectorial ion flow. Physiological imperfections in the coupling may be caused by two factors: (1) parallel pathways of ion flow (leaks) and (2) intrinsic uncoupling within the pumps. Many workers assume that ion pumps are completely coupled and that all uncoupling may be attributed to external leaks. Actually there is no thermodynamic or kinetic justification for such an assumption. Recently, a number of reports have appeared showing that a certain degree of intrinsic uncoupling is indeed present in ion pumps and transport systems.

Passive pump-mediated (ouabain-sensitive) Rb^+ fluxes in the absence of ATP and phosphate have been measured in phospholipid vesicles reconstituted with kidney (Na,K)ATPase (Karlish & Stein, 1982) and in gastric vesicles enriched in (H,K)ATPase (Soumarmon et al., 1984). It has been also reported that a (Na,K)ATPase-mediated Rb^+ uptake decoupled from Na^+ efflux can be induced in erythrocytes by applying an alternating current (ac) field in the range of 20 V/cm (Serpersu & Tsong, 1984). The anion transporter of the human red cell membrane, whose physiological function is a one-to-one exchange transport of extracellular with intracellular anions, also mediates net anion efflux (Knauf et al., 1977). This efflux is the result of intrinsic uncoupling of the transporter (Frölich et al., 1983). A DCCD[1]-sensitive ATPase

† This study was supported by an EMBO short-term travel grant enabling D.P. to work in Rehovot.
‡ University of Padova.
§ The Weizmann Institute of Science.

0006-2960/86/0425-0767$01.50/0

activity catalyzed by CF_1–CF_0 but uncoupled from proton translocation has been characterized in chloroplasts (Pick, 1984). Intrinsic uncoupling of the ATPase in chloroplasts is also indicated by earlier studies showing a pump-mediated passive proton flow under nonphosphorylating conditions (Portis et al., 1975; Schonfeld & Neumann, 1977; Ho et al., 1979; Gräber et al., 1981). Branching of the photocycle of bacteriorhodopsin into coupled (pumping) and uncoupled (not pumping) pathways has been proposed by Westerhoff & Dancshâzy (1984) as the mechanism underlying the observed inhibition of proton pumping by the electrochemical potential difference for the protons $\Delta\tilde{\mu}_H$ (Westerhoff et al., 1979). Studies of the kinetics of ΔpH formation and decay in reconstituted purple membranes of halobacteria also indicate the existence of uncoupled $\Delta\tilde{\mu}_H$-controlled reaction cycles which result in a reduced proton pumping activity of the bacteriorhodopsin at increasing light intensities (Tu et al., 1981a; Ramirez et al., 1983).

We have proposed that the mitochondrial proton pumps also are not completely coupled and have considered the typical relationship between the rate of the driving reaction (electron transfer or ATP hydrolysis) and $\Delta\tilde{\mu}_H$ at static head obtained by titrating with inhibitors to be a manifestation of intrinsic uncoupling (Pietrobon et al., 1981, 1983). The preceding paper in this issue (Zoratti et al., 1985) shows that the alternative explanations put forward, based on the non-ohmic conductance of the membrane to protons (Nicholls, 1974) and/or the uncoupled reaction rate of a certain amount of broken or damaged mitochondria (Duszynsky & Vojtczak, 1984), cannot account for the experimental observation.

Recently Pietrobon & Caplan (1985) have investigated the kinetic and thermodynamic properties of intrinsically uncoupled model systems, by simulating the flow–force relationships of a six-state model of a proton pump. Some of their results describing the regulation of intrinsic uncoupling by the thermodynamic forces (affinity of the driving reaction and $\Delta\tilde{\mu}_H$) are reported and discussed here. The same model, modified by introducing different kinds of inhibitors, is then used to simulate the relationships between rate of electron transfer and $\Delta\tilde{\mu}_H$ at static head, both in the hypothetical limiting case that a nonzero rate is exclusively due to intrinsic uncoupling (no leaks) and in the more physiological case of mixed extrinsic and intrinsic uncoupling as found in the preceding paper (Zoratti et al., 1985). The rate of electron transfer can be varied by varying the concentration of substrate instead of by using an inhibitor: experiments and corresponding simulations are also presented for this case. The simulations show that the observed behavior may indeed be a manifestation of intrinsic uncoupling in the mitochondrial proton pumps. The physiological significance of this conclusion and its implications for the correct analysis of measurements of the stoichiometry of coupled processes are discussed.

Results

Figure 1 shows the six-state model of a proton pump described in Pietrobon & Caplan (1985). We shall use this model here to compare simulated behavior with experimental results such as those presented in the preceding paper (Zoratti et al., 1985), relating to the electron transfer from succinate to O_2 in rat liver mitochondria. In this case S represents succinate and P corresponds to the products of succinate oxidation (fumarate and H^+), and the transitions between states 4 and 5 are "reduced" (Hill, 1977) from a prior reaction scheme comprising intervening transient states involved in the reaction with O_2 (Pietrobon & Caplan, 1985). The reaction scheme in Figure 1 gives rise to sigmoidal flow–force relationships (Pietrobon & Caplan, 1985). Using the Hill diagram method to derive the kinetic equations (Hill, 1977), we have studied how these flow–force relationships are modified by intrinsic uncoupling.

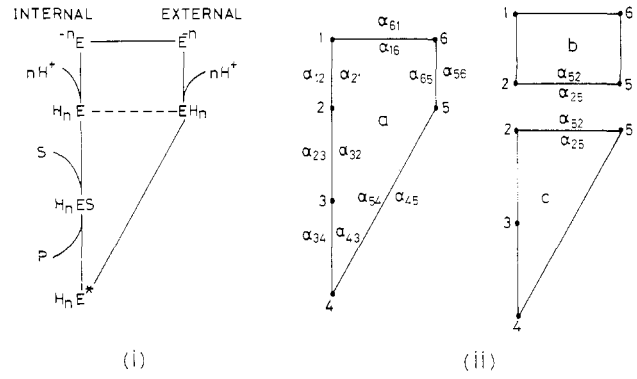

FIGURE 1: Six-state model of a proton pump. (i) Complete diagram. E is a membrane-bound protein with n negatively charged proton binding sites accessible either to the internal medium or to the external medium. The reaction S → P brings about a conformational change in E to E*, in which state it undergoes a transition that changes the accessibility of the bound protons from the internal to the external medium. The transition indicated by a dashed line introduces the possibility of uncoupled cycles (slips). (ii) The cycles of the diagram: cycle a, completely coupled cycle; cycle b, proton slip cycle; cycle c, reaction slip cycle. The states are assigned numbers, and the α_{ij} are first-order or pseudo-first-order rate constants: $\alpha_{23} = \alpha_{23}{}^*c_s$, $\alpha_{16} = \alpha_{16}(0)\exp[-(nF/2RT)\Delta\psi_m]$, and $\alpha_{61} = \alpha_{61}(0)\exp[(nF/RT)\Delta\psi_m]$, where $\Delta\psi_m$ is the electrical potential difference between the planes in the membrane corresponding to the positions of the n empty binding sites in states 1 and 6. With n higher than 1, the transitions 1–2 and 5–6 are actually "reduced" transitions (Hill, 1977) involving a number of intervening transient states. The corresponding pseudo-first-order rate constants are hence complex functions of the proton concentration and the rate constants of the elementary transitions. If the reaction gives rise to more than one product, the transitions between states 3 and 4 are reduced transitions, and the rate constants are functions of those of the elementary transitions and the product concentrations. For more details, see Pietrobon & Caplan (1985).

Panels a and b of Figure 2 show simulations of the rates of electron transfer J_e and proton translocation J_H, respectively, as functions of $\Delta\tilde{\mu}_H$. $\Delta\tilde{\mu}_H$ is varied by varying $\Delta\psi$ while ΔpH and the concentrations of substrates and products are kept constant at the values prevailing under the experimental conditions of Pietrobon et al. (1982). Curves a correspond to very low values of the rate constants α_{25} and α_{52}, so that essentially only coupled cycle a operates (complete coupling, $q = 1$). The other curves (b–e) correspond to increasing values of these rate constants so that the contribution of uncoupled cycles b and c becomes more and more significant (intrinsic uncoupling, $q < 1$). The rate constants used in the simulations are chosen so as to give rise to a kinetically irreversible pump characterized by the following parameters close to those determined experimentally in Pietrobon et al. (1982): the flow controlling ranges of $\Delta\tilde{\mu}_H$, and the values of the flows and of $(L_{eH}/L_{He})^{eff}$ (Pietrobon & Caplan, 1985).[2]

The increase of J_e in the various sigmoidal flow–force curves of Figure 2a with increasing intrinsic uncoupling primarily

[1] Abbreviations: EGTA, [ethylenebis(oxyethylenenitrilo)]tetraacetic acid; Mops, 4-morpholinepropanesulfonic acid; TPMP, triphenylmethylphosphonium; Tris, tris(hydroxymethyl)aminomethane; PRCR, pump rate control ratio; q, degree of coupling; DCCD, N,N'-dicyclohexylcarbodiimide; FCCP, carbonyl cyanide p-(trifluoromethoxy)-phenylhydrazone.

[2] $(L_{eH}/L_{He})^{eff}$ is the ratio between the slope of the linear range of the curve J_e vs. $\Delta\tilde{\mu}_H$ at constant affinity A and the intercept of the linear range of J_H vs. $\Delta\tilde{\mu}_H$ at constant A divided by A.

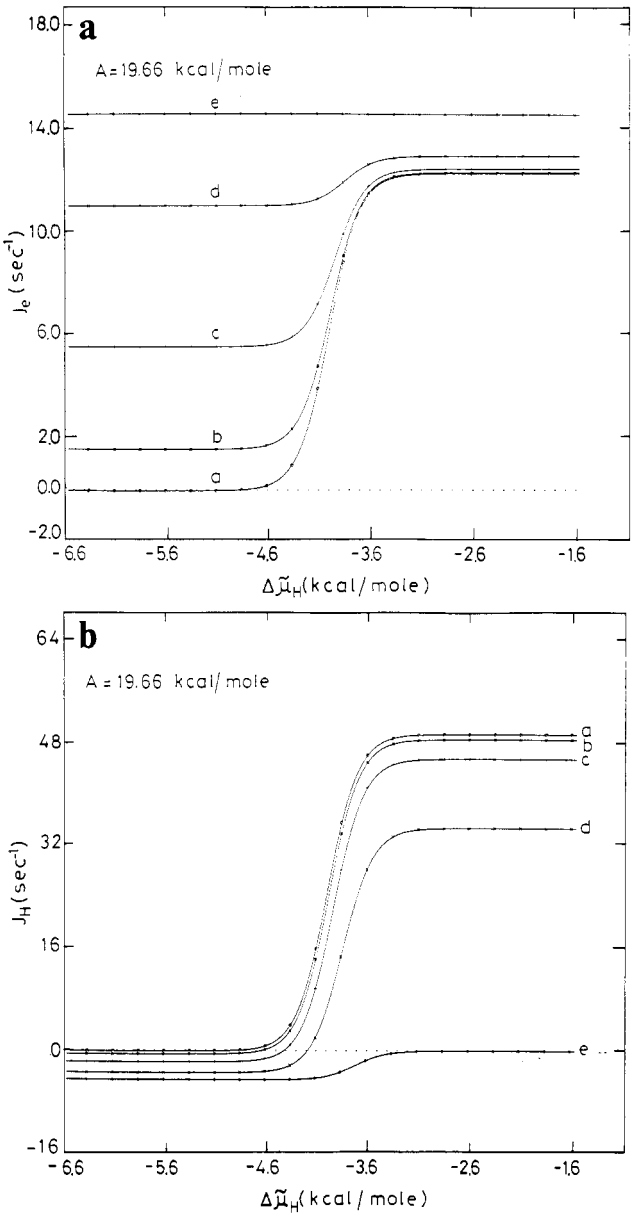

FIGURE 2: Simulated dependence of the rate of electron transfer J_e (a) and of proton translocation J_H (b) on $\Delta\tilde{\mu}_H$ at a constant value of the affinity A of the redox reaction. Families of curves correspond to increasing α_{52} and α_{25} with a degree of coupling varying from 1 (curves a) to 0 (curves e). $\Delta\tilde{\mu}_H$ is varied by varying $\Delta\psi$. The affinity A corresponds to the transfer of a single electron: $A = RT \ln K(c_{succ}/c_{fum})^{1/2}$ where $K = 1.31 \times 10^{13}$ M (at pH = 7.4 and P_{O_2} = 0.2 atm), c_{succ} = 20 mM, and c_{fum} = 0.05 mM. The parameters of the simulation are as follows: $n = 4$, $pH_{in} = pH_{ex} = 7.4$, $\Delta\psi_b^{in} = 0$, $\Delta\psi_b^{ex} = -50$ mV, $\alpha_{12} = 4 \times 10^2$ s^{-1}, $\alpha_{21} = 5$ s^{-1}, $\alpha_{32} = 8 \times 10^4$ s^{-1}, $\alpha_{34} = 4 \times 10^2$ s^{-1}, $\alpha_{43} = 4 \times 10^2$ s^{-1}, $\alpha_{45} = 40$ s^{-1}, $\alpha_{54} = 0.4$ s^{-1}, $\alpha_{56} = 10^2$ s^{-1}, $\alpha_{65} = 10^5$ s^{-1}, $\alpha_{23} = 1 \times 10^6$ M$^{-1/2}$ s^{-1}, $\alpha_{16}(0) = 1.3 \times 10^2$ s^{-1}, $\alpha_{61}(0) = 10^{12}$ s^{-1}. The values of α_{25} and α_{52} (in s^{-1}), respectively, in going from curves a to curves e are as follows: (a) 6.75×10^{-33}, 1×10^{-20}; (b) 1.36×10^{-12}, 2; (c) 6.75×10^{-12}, 10; (d) 3.375×10^{-11}, 50; (e) 6.75×10^{-1}, 1×10^{12}. $\Delta\psi_b^{in}$ and $\Delta\psi_b^{ex}$ represent phase-boundary potentials.

reflects the contribution of cycle c, the redox slip. It is seen that this contribution increases as $|\Delta\tilde{\mu}_H|$ increases. Figure 3 shows how the redox slip, i.e., the number of cycles c completed in unit time (cycle flux c in the Hill terminology) J_c, is regulated by $\Delta\tilde{\mu}_H$. The higher the force against which the pump moves protons (which means in the model the lower the rate constant α_{61} and the higher α_{16}), the higher the probability of redox slip, i.e., the higher the probability of cycle c with respect to that of cycle a. The two cycles can be regarded as

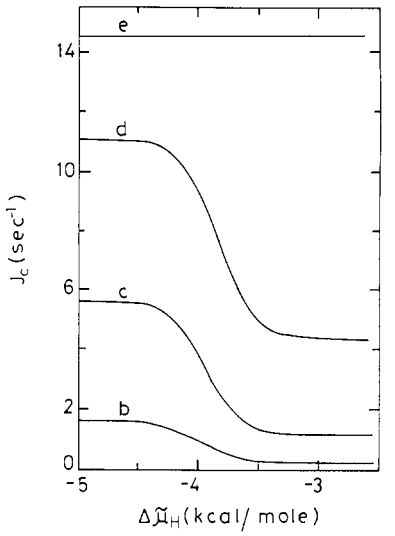

FIGURE 3: Redox slip (cycle flux J_c) as a function of $\Delta\tilde{\mu}_H$ for degrees of coupling corresponding to curves b–e of Figure 2.

in competition with each other. Thus the decrease in J_H at low $|\Delta\tilde{\mu}_H|$ in Figure 2b as intrinsic uncoupling increases reflects primarily a decreasing probability of coupled cycle a as a consequence of such competition. At high $|\Delta\tilde{\mu}_H|$ negative values of J_H appear due to the contribution of the proton slip (cycle b). Below a threshold $|\Delta\tilde{\mu}_H|$ value the proton slip is zero as can be seen from curve e, which represents the completely uncoupled pump ($q = 0$).

Figure 4 shows J_e and J_H as functions of A at constant $\Delta\tilde{\mu}_H$ for different degrees of coupling varying from 1 (curves a) to 0 (curves e). Comparison between the two curves e ($q = 0$) in panels a and b of Figure 4, which show how cycle fluxes c (redox slip) and b (proton slip), respectively, depend on the affinity, indicates that the two uncoupled cycles also compete with each other. Their relative probability is controlled by the affinity: as A decreases, the reaction slip decreases while the proton slip increases. In the saturated region at high affinity only the reaction slip occurs, while in the saturated region at low affinity only the proton slip occurs. At the high value of the affinity in Figure 2 redox slip is by far the main uncoupled cycle.

Figure 5 shows the normalized flow ratio J_H/nJ_e as a function of the normalized force ratio $n\Delta\tilde{\mu}_H/A$ (A is constant, $\Delta\tilde{\mu}_H$ is varied by varying $\Delta\psi$ as in Figure 2) for different degrees of coupling of the pump. For the completely coupled pump ($q = 1$, curve a) $J_H = nJ_e$ for all values of $\Delta\tilde{\mu}_H$. When the contributions of the uncoupled cycles become significant, this stoichiometric relationship between J_e and J_H no longer exists. Instead, the flow ratio depends on $\Delta\tilde{\mu}_H$. Its maximum value at low $|\Delta\tilde{\mu}_H|$ is lower than n, the deviation from n being determined by the degree of intrinsic uncoupling. Its value at $\Delta\tilde{\mu}_H = 0$ (level flow), J_H/J_e^{lf}, is always, even for high values of the forces, equal to $q^{ons}Z^{ons}$ (Caplan, 1981) where q^{ons} and Z^{ons} are the degree of coupling and the phenomenological stoichiometry in the Onsager region close to equilibrium (A and $n|\Delta\tilde{\mu}_H| \ll RT$) (Kedem & Caplan, 1965). Note that $\Delta\tilde{\mu}_H = 0$ need not actually be attained in order to determine J_H/J_e^{lf} since as $\Delta\tilde{\mu}_H$ approaches zero the flow ratio becomes constant. When $q^{ons} < 1$ the state at which $J_H = 0$ (see Figure 2b) is no longer an equilibrium state but rather a static head, with $J_e^{sh} > 0$ increasing as intrinsic uncoupling increases (see Figure 2a) and $|\Delta\tilde{\mu}_H^{sh}| < A/n$ decreasing as intrinsic uncoupling increases.

Let us consider the case corresponding to curve b in Figure 2b (with $J_e^{sh} = 1.72$ s^{-1} and $\Delta\tilde{\mu}_H^{sh} = -4.64$ kcal/mol) and see

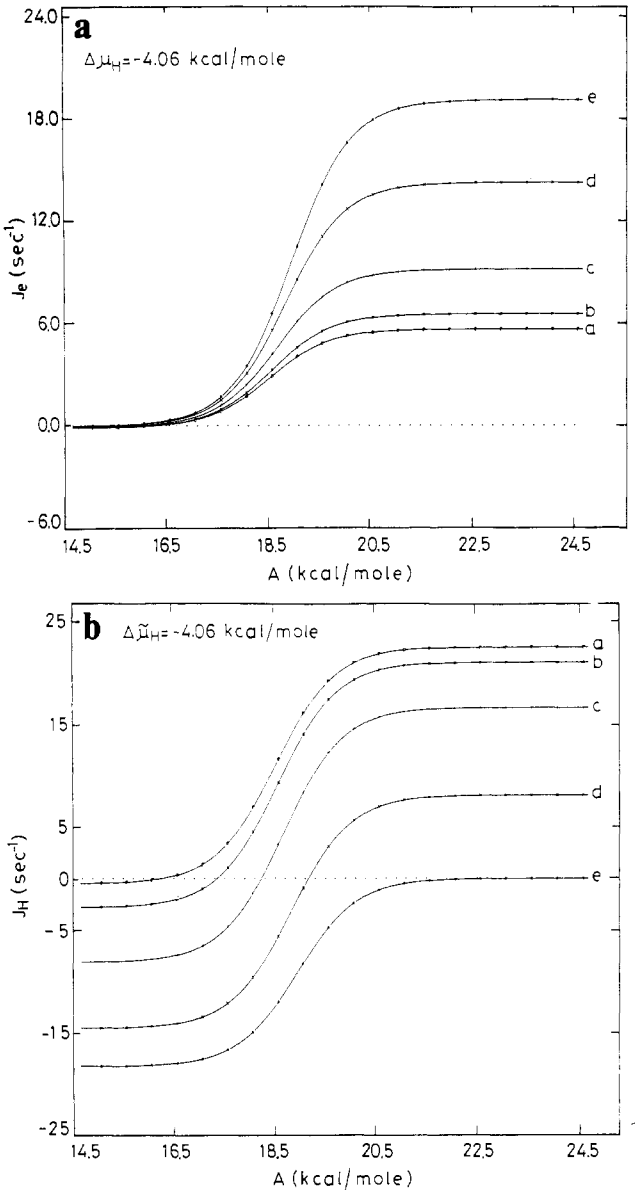

FIGURE 4: Simulated dependence of J_e (a) and J_H (b) on A at a constant value of $\Delta\tilde{\mu}_H$. Families of curves correspond to increasing α_{52} and α_{25} with degrees of coupling varying from 1 (curves a) to 0 (curves e). A is varied by varying the substrate concentration c_{succ}. Parameters of the simulation are as in Figure 2.

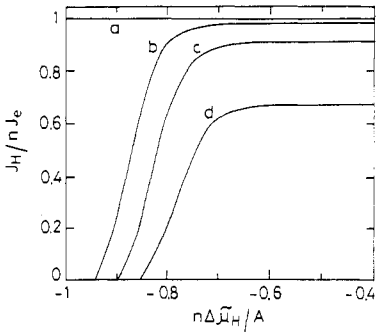

FIGURE 5: Dependence of the normalized flow ratio $J_H/J_e n$ on the normalized force ratio $n\Delta\tilde{\mu}_H/A$ for degrees of coupling corresponding to curves a–d of Figure 2. A = 19.66 kcal/mol.

what kind of relationship between J_e^{sh} and $\Delta\tilde{\mu}_H^{sh}$ is obtained when the slipping pump is progressively inhibited.

There are different possible ways of introducing the effect of an inhibitor in the model of Figure 1. One possibility is that the inhibitor binds with the same affinity to all the enzymatic states in the reaction cycle (alternatively, it binds preferentially to one or more of the states in the cycle). Binding is considered to be at equilibrium. As an example consider state 2 (EH_n), which binds inhibitor I at concentration c_I to give state 2′ (EH_nI):

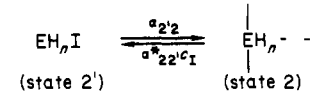

If binding is at equilibrium, state 2 in the reaction cycle is actually a mixture of states 2 and 2′; the fraction of state 2 in the mixture is given by

$$\theta = \alpha_{2'2}/(\alpha_{2'2} + \alpha^*_{22'}c_I)$$

Since only the fraction of enzyme molecules in state 2 can undergo the transitions 2–1, 2–3, and 2–5 in the reaction cycle, the rate constants α_{21}, α_{23}, and α_{25} become multiplied in the presence of inhibitor by the factor θ varying from 1 (at zero inhibitor concentration) to 0 (at very high inhibitor concentration). Thus an inhibitor that binds with the same affinity to all the states in the cycle decreases the population of the states and hence all the rate constants by a factor proportional to the inhibitor concentration. This is actually equivalent to a reduction of the number of enzymes by the same factor.

When the slipping pump that gives rise to curve b in Figure 2 is progressively inhibited with an inhibitor of this kind (inhibitor 1), the simulated relationship between J_e^{sh} and $\Delta\tilde{\mu}_H^{sh}$ is given by straight line 1 in Figure 6 (inhibition of J_e without change in $\Delta\tilde{\mu}_H$). The coupled and uncoupled cycles are inhibited simultaneously to the same extent, thus leaving $\Delta\tilde{\mu}_H$ unchanged. The same line is obtained whether the inhibitor binds only to state 2 or to any other state in the cycle.

A different type of inhibitor may, on binding, reduce to practically zero (or anyway modify) the rate constants of one or more transitions in the cycle. We have simulated in particular the case in which the rate constants α_{23} and α_{32} (of the substrate binding transition) are reduced by a factor of 10^{20} in a fraction of the enzyme molecules proportional to the inhibitor concentration. The remaining fraction is unaffected.

Such an inhibitor (inhibitor 2) gives rise to curve 2 in Figure 6. The different behavior arises from the fact that in the

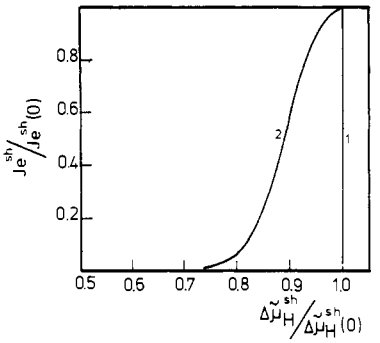

FIGURE 6: Simulated relationships between J_e^{sh} and $\Delta\tilde{\mu}_H^{sh}$ upon progressive inhibition of a slipping proton pump with two kinds of inhibitors. Parameters of the simulation are as in Figure 2 with $\alpha_{25} = 1.35 \times 10^{-12}$ and $\alpha_{52} = 2$. Curve 1 is obtained by multiplying all the rate constants by a factor varying from 1 (at zero inhibitor concentration) to 0. Curve 2 is obtained by considering an increasing fraction θ of the enzymes with rate constants α_{23} and α_{32} decreased by a factor of 10^{20} ($\theta = 0$ at zero inhibitor concentration). The same curve 2 is also obtained by decreasing the affinity of the redox reaction by varying c_{succ}. See text for further details. $\Delta\tilde{\mu}_H^{sh}(0)$ is the value of $\Delta\tilde{\mu}_H$ at which $J_H = 0$ in the flow–force curve b of Figure 2b (zero inhibitor concentration). $J_e^{sh}(0)$ is the value of J_e corresponding to $\Delta\tilde{\mu}_H^{sh}(0)$ in the flow–force curve b of Figure 2a. $\Delta\tilde{\mu}_H^{sh}(0) = -4.64$ kcal/mol; $J_e^{sh}(0) = 1.72$ s^{-1}.

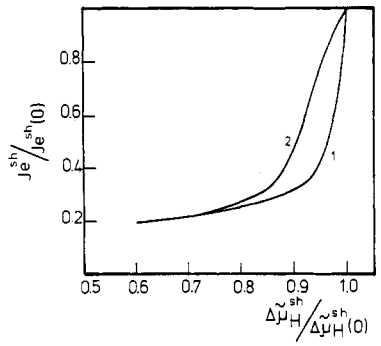

FIGURE 7: Simulated relationships between J_e^{sh} and $\Delta\tilde{\mu}_H^{sh}$ upon progressive inhibition of a slipping proton pump with a constant proton-"leak" conductance L_H^l in parallel. $L_H^l = 0.5$ mol kcal^{-1} s^{-1}. Simulations 1 and 2 and parameters are as in Figure 5, but $\alpha_{25} = 9.45 \times 10^{-13}$ s^{-1} and $\alpha_{52} = 1.4$ s^{-1}. $\Delta\tilde{\mu}_H^{sh}(0) = -4.41$ kcal/mol; $J_e^{sh}(0) = 1.75$ s^{-1}.

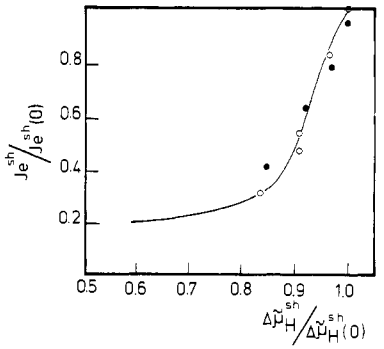

FIGURE 8: Relationship between J_e^{sh} and $\Delta\tilde{\mu}_H^{sh}$ in rat liver mitochondria. The electron transfer is varied by adding increasing concentrations (from 0 to 15 mM) of malonate (○) or by decreasing the concentration of succinate from 20 mM to 25 μM (●). The medium composition was as follows: 0.2 M sucrose, 20 mM Tris/Mops, 2 mM P_i/Tris, 0.5 mM EGTA, 5 μM rotenone, 5 mM glycerol, and 1 μg/mg oligomycin, pH 7.4; $T = 25$ °C. Mitochondria (2 mg/mL) were incubated for 7 min, after which 50 μM fumarate, 215 μM malate, and 20 mM succinate (○) or succinate varying from 20 mM to 25 μM (●) was added. After 30 s the O_2 consumption and $\Delta\tilde{\mu}_H$ were measured as described in the preceding paper (Zoratti et al., 1985). The concentration of malate added is that in equilibrium with 50 μM fumarate, assuming an equilibrium constant of 4.3 for the fumarate hydrase reaction. The values of the affinities for electron transfer from succinate to oxygen, calculated as $A = RT \ln K(c_{succ}/c_{fum})^{1/2}$ (where $K = 1.31 \times 10^{13}$ at pH = 7.4 and $P_{O_2} = 0.2$ atm), are $A = 19.66$ kcal/mol (○) and $A = 19.66 - 17.68$ kcal/mol (●). $J_e^{sh}(0) = 28$ nmol of e/(min·mg); $\Delta\tilde{\mu}_H^{sh}(0) = -4.5$ kcal/mol. The curve shown in the figure is the simulated relationship (curve 2 in Figure 7).

fraction of inhibited pumps, while coupled cycle a and the redox slip (cycle c) are reduced to zero, the proton slip (cycle b) is not inhibited. On the contrary, it is increased with respect to the noninhibited fraction, due to the release of the competition between cycles a, b, and c. At the beginning of the titration increasing inhibition gives rise to increasing proton slip and consequently a decrease in $|\Delta\tilde{\mu}_H|$. As mentioned above, the proton slip itself depends on $\Delta\tilde{\mu}_H$ (see Figure 2b, curve e), and below a threshold $|\Delta\tilde{\mu}_H|$ value it becomes practically zero.

Exactly the same behavior (curve 2) is obtained when the reaction rate is varied by decreasing the concentration of substrate. Again, the reason is the competition among the possible cycles: a decrease in the concentration of substrate, and therefore in the affinity of the reaction, decreases the probability of the coupled cycle and of the redox slip while it relatively increases that of the proton slip (cf. the regulation by the forces of the relative contribution of the two kinds of slip).

The behavior in Figure 6 is obtained when the nonzero rate of electron transfer at static head is exclusively due to intrinsic uncoupling. However, in mitochondria extrinsic uncoupling due to a parallel pathway for proton flow is certainly present, since the membrane has a finite permeability to protons (leaks). It is clear that if the pumps are completely coupled and the nonzero rate of electron transfer at static head is due only to extrinsic leaks, the relationship between J_e^{sh} and $\Delta\tilde{\mu}_H^{sh}$, when the pumps are progressively inhibited, simply reflects that between the parallel pathway and $\Delta\tilde{\mu}_H$.

The preceding paper (Zoratti et al., 1985) has shown that, in rat liver mitochondria oxidizing succinate, about 30% of the rate of electron transfer at static head without inhibitor is accounted for by the influx of protons through leaks. We have proposed that the rest of electron transfer is due to intrinsic uncoupling of the redox proton pumps. Figure 7 shows the simulated relationships between J_e^{sh} and $\Delta\tilde{\mu}_H^{sh}$ upon inhibition with the two different kinds of inhibitors discussed above, for the case of a constant proton-leak conductance of the same order of magnitude as that measured experimentally added in parallel to the pumps. The rate constants α_{25} and α_{52} are chosen so that about 30% of J_e^{sh} at zero inhibitor concentration is accounted for by the leak and the rest by intrinsic uncoupling. Curve 1 is again obtained with inhibitor 1; curve 2 is obtained with inhibitor 2 or by varying the substrate concentration. The different simulated behavior obtained with the two hypothetical inhibitors is strongly reminiscent of the different experimental results found in rat liver mitochondria with the two inhibitors antimycin and malonate [cf. Figure 7 in the preceding paper (Zoratti et al., 1985) and also Pietrobon et al. (1981)]. We have pointed out that the same simulated curve 2 is given by the model both on varying the substrate concentration and on adding inhibitor 2. Figure 8 shows that in rat liver mitochondria, also, the same relationship between J_e^{sh} and $\Delta\tilde{\mu}_H^{sh}$ is obtained either by varying the succinate concentration or by varying the malonate concentration. Note that not only the shape but also the values of J_e^{sh} and $\Delta\tilde{\mu}_H^{sh}$ without inhibitor in the simulations are rather close to the experimental ones: $J_e^{sh}(0) = 1.75$ s^{-1}, which corresponds to 21.1 nmol of e/(mg·min), assuming 0.2 nmol of pump/mg, and $\Delta\tilde{\mu}_H^{sh}(0) = -4.41$ kcal/mol.

From the comparison between simulated behavior and experimental results one can therefore conclude that the typical relationship between J_e^{sh} and $\Delta\tilde{\mu}_H^{sh}$ could indeed be a manifestation of intrinsic uncoupling. Moreover, the simulations confirm earlier suggestions (Pietrobon et al., 1981) that (1) while antimycin inhibits both proton slip and redox slip together with the coupled cycle, malonate does not inhibit proton slip, thus accounting for the different behavior, and (2) redox slip is the main uncoupled cycle in mitochondrial redox proton pumps at high affinity.

Another way of looking at the problem of intrinsic uncoupling is to consider, instead of a homogeneous population of pumps with a certain degree of intrinsic uncoupling as an integral part of their catalytic mechanism, a certain subpopulation of pumps that are totally uncoupled among a population of completely coupled ones. The totally uncoupled pumps can be simulated by increasing the rate constants α_{25} and α_{52} so that the probability of coupled cycle a becomes insignificant with respect to that of uncoupled cycles b and c ($q = 0$). At the high value of the affinity considered by us cycle c is the main uncoupled cycle, and the totally uncoupled pumps transfer electrons without pumping protons most of the time, only occasionally acting as proton translocators. When an increasing fraction of the completely coupled pumps becomes totally uncoupled, the flow–force curves are modified

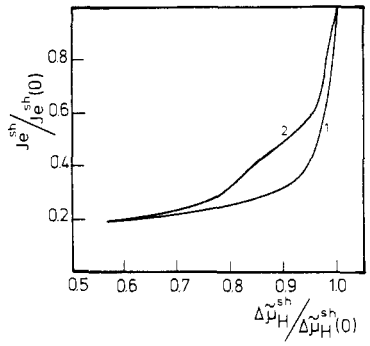

FIGURE 9: Simulated relationships between J_e^{sh} and $\Delta\tilde{\mu}_H^{sh}$ upon progressive inhibition of a fraction (0.92) of completely coupled pumps ($q = 1$) and a fraction (0.08) of totally uncoupled pumps ($q = 0$) with a constant proton-leak conductance L_H^l in parallel. $L_H^l = 0.5$ mol kcal^{-1} s^{-1}. Simulations 1 and 2 and parameters are as in Figure 5, but $\alpha_{25} = 6.75 \times 10^{-33}$ s^{-1} and $\alpha_{52} = 1 \times 10^{-20}$ s^{-1} for the fraction of completely coupled pumps, and $\alpha_{25} = 6.75 \times 10^{-1}$ s^{-1} and $\alpha_{52} = 1 \times 10^{12}$ s^{-1} for the fraction of totally uncoupled pumps. $\Delta\tilde{\mu}_H^{sh}(0) = -4.41$ kcal/mol; $J_e^{sh}(0) = 1.82$ s^{-1}.

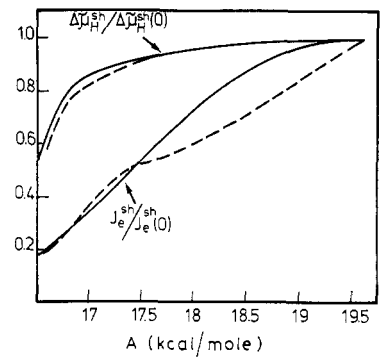

FIGURE 10: Simulated dependence of J_e^{sh} and $\Delta\tilde{\mu}_H^{sh}$ on the affinity A. (—) Homogeneous population of slipping pumps ($\alpha_{25} = 9.45 \times 10^{-13}$ s^{-1}, $\alpha_{52} = 1.4$ s^{-1}) with a constant proton-leak conductance in parallel ($L_H^l = 0.5$ nmol kcal^{-1} s^{-1}). $\Delta\tilde{\mu}_H^{sh}(0) = -4.41$ kcal/mol; $J_e^{sh}(0) = 1.75$ s^{-1}. (--) Fraction (0.08) of totally uncoupled pumps ($\alpha_{25} = 0.675$ s^{-1}, $\alpha_{52} = 1 \times 10^{12}$ s^{-1}) with a constant proton-leak conductance in parallel ($L_H^l = 0.5$ nmol kcal^{-1} s^{-1}). The other fraction (0.92) of pumps is completely coupled ($\alpha_{25} = 6.75 \times 10^{-33}$ s^{-1}, $\alpha_{52} = 1 \times 10^{-20}$ s^{-1}). $\Delta\tilde{\mu}_H^{sh}(0) = -4.41$ kcal/mol; $J_e^{sh}(0) = 1.82$ s^{-1}. A is varied by varying the succinate concentration.

in a similar manner (not shown) to that depicted in Figure 2, which refers to increasing intrinsic uncoupling in all the pumps. However, in the case of totally uncoupled pumps the uncoupled electron flow is not controlled by $\Delta\tilde{\mu}_H$ in contrast to the redox slip (cf. curve e with curves b–d in Figure 3).

Figure 9 shows simulations analogous to those of Figure 7 where, instead of considering a certain degree of intrinsic uncoupling in all the pumps, a certain fraction of the pumps is totally uncoupled. The addition of inhibitor 1, which decreases the number of coupled and uncoupled pumps to the same extent, results in behavior identical with that obtained with slipping pumps (curve 1). As before, inhibitor 2 (or a change in substrate concentration) gives rise to different behavior (curve 2). A decrease in substrate concentration not only decreases electron transfer in totally uncoupled pumps but also, since the two cycles b and c compete with each other, changes the relative contribution of the two uncoupled cycles in favor of cycle b. Analogously, the subpopulation of totally uncoupled pumps inhibited by inhibitor 2 does not transfer electrons but still catalyzes downhill proton translocation (at a higher rate). The strange shape of curve 2 in Figure 9 probably arises from the fact that in the earlier part of the titration the decrease in uncoupled electron flow is more significant than the increase in uncoupled proton flow, while the opposite is true in the central part.

The simulations in Figures 7 and 9 show somewhat different behavior with the two kinds of intrinsic uncoupling discussed above only when either inhibitor 2 or a change in the substrate concentration is used to vary the activity of the pumps. Figure 8 shows that the experimental points are rather well simulated by the curve obtained with a homogeneous population of slipping pumps. However, in view of the scatter, a discrimination between the two cases on the basis of this kind of experiment alone appears difficult. The simulations in Figure 10 suggest another possible method of discriminating between the two cases. They show $\Delta\tilde{\mu}_H$ and the rate of electron transfer at static head as functions of the affinity of the redox reaction for the two kinds of intrinsic uncoupling. Figure 11 shows the corresponding results in rat liver mitochondria. The different simulated behavior of J_e^{sh} vs. A obtained with a homogeneous population of slipping pumps (solid line in Figure 10) and with a subpopulation of totally uncoupled pumps (dashed line) arises from the different sensitivity to the substrate concentration of the totally uncoupled and slipping pumps at high values of $|\Delta\tilde{\mu}_H|$ (cf. Figure 4a, curves b and e). A similar difference

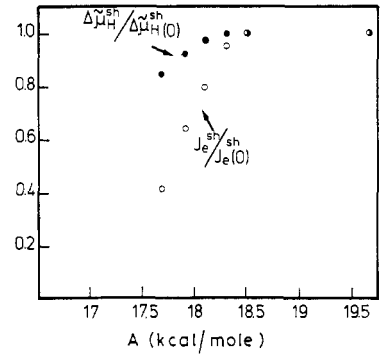

FIGURE 11: Dependence of J_e^{sh} (○) and $\Delta\tilde{\mu}_H^{sh}$ (●) on the affinity in rat liver mitochondria. The medium composition and procedure were as in Figure 8. A is varied by varying the succinate concentration and is calculated as in the legend to Figure 8.

in sensitivity to the substrate concentration for coupled and uncoupled electron transfer in mitochondria is shown in Figure 8 of the preceding paper (Zoratti et al., 1985). Consequently, comparison of the results of Figure 11 with the simulations of Figure 10 suggests that intrinsic uncoupling in mitochondrial proton pumps is due to a homogeneous population of pumps with a certain degree of intrinsic uncoupling, rather than to a subpopulation of totally uncoupled pumps.

Discussion

Intrinsic uncoupling differs from extrinsic uncoupling (leaks or parallel pathways) in that it is dependent per se on the machinery that couples the two processes. Considering a slipping redox proton pump as an example, the rate of uncoupled electron transfer (redox slip) or that of uncoupled downhill proton translocation (proton slip) are not independent of the rate of the coupled reaction since they are all catalyzed by the same enzyme. Intrinsic uncoupling therefore depends on the overall kinetic parameters of the pump and is regulated by both thermodynamic forces, the affinity of the reaction and $\Delta\tilde{\mu}_H$.

Near-equilibrium nonequilibrium thermodynamics allows a phenomenological description of intrinsically uncoupled systems (operating close to equilibrium in the Onsager region) in terms of linear flow–force relationships and their characteristic parameters: the degree of coupling, q^{ons}, and the phenomenological stoichiometry, Z^{ons}. This approach has been

previously used to describe the mitochondrial redox proton pumps (Pietrobon et al., 1982; Walz, 1983) and to conclude that they are not completely coupled. Pietrobon & Caplan (1985) have recently pointed out the limitations of such an approach when applied to regions of linearity far from equilibrium [cf. also Westerhoff (1983)], in particular because q in such regions is itself dependent on the values of the forces. Modeling studies then become crucial for the elucidation of the thermodynamic and kinetic properties of intrinsically uncoupled systems. The Hill diagram method, which enables one to write down at sight the steady-state kinetic equations relating the flows to the thermodynamic forces for any cyclic or multicyclic enzymatic reaction scheme, greatly facilitates such a study (Hill, 1977).

The analysis of how the flow–force relationships of the proton pump model shown in Figure 1 are modified by intrinsic uncoupling shows that the thermodynamic forces determine both the relative contributions and the magnitude of uncoupled cycles c (reaction slip) and b (proton slip). As the affinity of the reaction increases, the reaction slip increases while the proton slip decreases. As $|\Delta\tilde{\mu}_H|$ increases, both the proton slip *and* the reaction slip increase. To the extent that the contribution of one or the other uncoupled cycle is increased, the contribution of the fully coupled cycle is decreased due to the competition between uncoupled and coupled cycles.

Any real proton pump is probably characterized by a much more complicated reaction scheme. However, the basic result of a competition between the possible coupled and uncoupled cycles regulated by kinetic parameters such as the concentrations of reactants and products, the concentration of the transported ion, $\Delta\psi$, and any other modulator of the enzymatic activity remains valid for any model.

Some degree of slip, however slight, may be inevitable in any pump mechanism. However, intrinsic uncoupling may actually play an important regulatory role in the operation of the pump. The regulation of intrinsic uncoupling characteristic of the simple model studied may well have physiological significance for the efficiency of oxidative phosphorylation. Particularly significant aspects are the steep dependence of the proton slip on $|\Delta\tilde{\mu}_H|$ and its sharp cutoff below a threshold value, as well as the regulation by $\Delta\tilde{\mu}_H$ of the reaction slip, which decreases as $|\Delta\tilde{\mu}_H|$ decreases. These properties would lead to an increase of the overall degree of coupling and efficiency of oxidative phosphorylation when an increased rate of phosphorylation is needed. On the other hand, they would prevent dangerously high values of $|\Delta\tilde{\mu}_H|$ from being reached (which could be detrimental to the integrity of the membrane). Another possible level of regulation of the slip can be achieved by specific physiological effectors that bind to the pump.

The data presented in the literature on the regulation of intrinsic uncoupling in the systems where it has been found are in accord with the predictions from models of the type considered by us. Net chloride efflux from intact erythrocytes, which arises from intrinsic uncoupling of the anion exchanger, is regulated by $\Delta\psi$ and by the external chloride concentration, increasing at low external concentration and at high $\Delta\psi$ (Frölich et al., 1983). The DCCD-sensitive ATPase activity in chloroplasts, catalyzed by CF_1–CF_0 but uncoupled from proton translocation, is Ca^{2+}-stimulated and $\Delta\tilde{\mu}_H$-dependent, increasing as $|\Delta\tilde{\mu}_H|$ increases above a threshold value (a slightly higher $|\Delta\tilde{\mu}_H|$ being necessary to activate the uncoupled reaction cycle as compared with that activating coupled ATP synthesis) (Pick, 1984). The proton slip of the ATPase indicated by earlier studies (see the introduction) in chloroplasts under nonphosphorylating conditions increases with light, i.e., with $|\Delta\tilde{\mu}_H|$, and is inhibited by the presence of adenine nucleotides. The relative contribution of the coupled and uncoupled reaction cycles in bacteriorhodopsin is regulated by $\Delta\tilde{\mu}_H$, the reaction slip increasing as $|\Delta\tilde{\mu}_H|$ increases (Tu et al., 1981a; Ramirez et al., 1983; Dancshâzy et al., 1984; Westerhoff & Dancshâzy, 1984). It has been suggested that, since the photoreaction proceeds at an essentially fixed rate, a $\Delta\tilde{\mu}_H$-controlled slip regulation might provide a "safety valve" (Caplan, 1982) and a way to ensure that the control of free energy transduction is at least partially by the $\Delta\tilde{\mu}_H$-driven processes and not only in the irreversible first transition of the pathway (Westerhoff & Dancshâzy, 1984).

The recognition of intrinsic uncoupling in the mitochondrial proton pumps, apart from the possible implications for the regulation of the efficiency of energy transduction, has interesting consequences for the interpretation of a number of typical bioenergetic measurements such as determinations of the stoichiometry of coupled processes. The view that uncoupling is uniquely an extrinsic property due to the permeability of the membrane leads to the conclusion that the measurement of the flow ratio at level flow, J_H/J_e^{lf}, (i.e., at $\Delta\tilde{\mu}_H = 0$, or also at $|\Delta\tilde{\mu}_H|$ higher than 0 if a highly non-ohmic proton conductance is assumed), provides the value of the mechanistic stoichiometry n for any pump or segment of the respiratory chain, irrespective of the value of the electron-transfer rate at static head. The view that uncoupling is also an intrinsic molecular property of the pumps introduces the concept that measurement of the flow ratio J_H/J_e at low values of $|\Delta\tilde{\mu}_H|$ always provides an underestimate of the mechanistic stoichiometry ($J_H/nJ_e^{lf} < 1$) and, more interestingly, the "normalized underestimate" J_H/nJ_e^{lf} reflects a molecular property that can be different for different pumps or segments of the respiratory chain.

For a correct comparative analysis of the results of flow ratio measurements it would be useful to find an operational parameter that for different pumps is uniquely related to, and therefore gives a measure of, the normalized underestimate J_H/nJ_e^{lf}. This parameter would also represent a common operational measure for the intrinsic uncoupling of different pumps [here and in the following discussion, "intrinsic uncoupling" is used with the broader meaning of partial uncoupling (slip) in a homogeneous population or total uncoupling in a subpopulation]. As discussed in the preceding paper (Zoratti et al., 1985), one of the arguments for intrinsic uncoupling in mitochondrial proton pumps stems from the observation of an electron transfer rate at static head in excess of that accounted for by the passive proton influx. However, different values of this "excess" reaction rate for different pumps do not necessarily mean different extents of intrinsic uncoupling and therefore different values of J_H/nJ_e^{lf}, since the reaction rate at static head can be different for different pumps simply because of different kinetic parameters. The ratio between the maximum reaction rate in the saturated region at low $|\Delta\tilde{\mu}_H|$ and the excess reaction rate at static head seems likely to be a better operational measure for the intrinsic uncoupling of different pumps. We call this ratio the pump rate control ratio PRCR. However, simulations with different sets of kinetic parameters show that the relationship between the PRCR and J_H/nJ_e^{lf} is not unique. Nevertheless, it is very similar for most cases, the differences between different pumps being mainly due to different relative contributions of the uncoupled cycles. The relationship is shown in Figure 12. Curve a is obtained when the PRCR is decreased by increasing the intrinsic uncoupling of a homogeneous population of slipping pumps, while curve b is obtained with an increasing

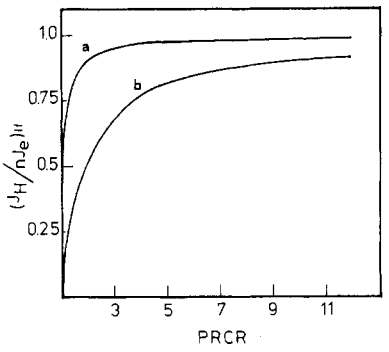

FIGURE 12: Normalized flow ratio as a function of pump rate control ratio, PRCR (see text for definition). (Curve a) PRCR varied by varying the degree of coupling in a homogeneous population of pumps. (Curve b) PRCR varied by varying the fraction of totally uncoupled pumps. The same curves (a) and (b) are obtained either by using the parameters of the simulation given in the legend to Figure 2 or by using a completely different set of parameters [as in Figure 5 of Pietrobon & Caplan (1985)].

fraction of totally uncoupled pumps. It is evident that the flow ratio at level flow is a negligible underestimate of the mechanistic stoichiometry n over an extended range of PRCRs for curve a (slipping pumps), while the underestimate becomes significant even for relatively high PRCRs for curve b (subpopulation of uncoupled pumps). The different behavior of the two kinds of intrinsic uncoupling arises essentially from the fact that the uncoupled electron flow of the subpopulation of totally uncoupled pumps is independent of $\Delta\tilde{\mu}_H$ (as would be that of a parallel pathway of electron transfer), while the slips are regulated by $\Delta\tilde{\mu}_H$ as shown in Figure 3.

The intrinsic uncoupling used in Figures 7 and 8 to simulate the experiments with succinate as substrate corresponds to a PRCR = 10 and to a $J_H/nJ_e^{lf} = 0.99$. The corresponding flow–force curve lies between curves a and b in Figures 2 and 4. The fraction of uncoupled pumps considered for the simulations of Figure 9 results in a PRCR = 10 and a $J_H/nJ_e^{lf} = 0.88$. Our data suggest that the excess respiration with succinate as substrate is due to molecular slipping in the pumps rather than to a subpopulation of totally uncoupled pumps or to a parallel pathway of electron flow. The flow ratio measured with this substrate at low values of $|\Delta\tilde{\mu}_H|$ is therefore probably a good estimate of the mechanistic stoichiometry. The much higher electron flow at static head and especially the much lower PRCR found with substrates of cytochrome oxidase such as tetramethylphenylenediamine (TMPD) or ferrocyanide (Azzone et al., 1985) (probably due to the existence of parallel pathways of electron transfer) suggest the possibility in this case of significant underestimation of the mechanistic stoichiometry by the measured flow ratio.

The fact that most of the electron flow at static head is due to intrinsic uncoupling also has consequences for the correct analysis of P/O measurements. In the presence of a $\Delta\tilde{\mu}_H$-regulated slip in the proton pumps the ratio closest to the mechanistic stoichiometry is that between the amount of ADP added and the total oxygen consumed during state 3, while in the presence of parallel pathways of electron flow or of totally uncoupled pumps it is that between the amount of ADP added and the oxygen consumed in excess of state 4 respiration.

The recognition of a certain degree of "physiological" intrinsic uncoupling in the proton pumps gives a new perspective also in the analysis of the unphysiological uncoupling induced by certain agents or conditions. Thus an induced increase in the intrinsic uncoupling of the proton pumps needs to be invoked to explain the differential effect of DCCD [see for a review Azzi et al. (1984)] or of fluorescamine (Tu et al., 1981b) on the proton pumping and electron transfer activities of cytochrome oxidase and the b–c_1 complex (J_e being practically unaffected while J_H is strongly inhibited), and the analogous differential effect on removal of subunit III of cytochrome oxidase (Pentilla, 1983) or on incubating beef heart cytochrome oxidase at 43–45 °C (Sone & Nicholls, 1984). Extrinsic uncoupling at the level of the membrane cannot explain the results since in all cases it was shown that there was negligible or zero increase in the proton membrane conductance. We have evidence that classical protonophoric agents also such as FCCP or gramicidin not only increase the proton membrane conductance but also behave as if in addition they intrinsically uncouple the pumps (Pietrobon & Zoratti, 1982 and unpublished experiments; Walz, 1983).

The analysis of the experiments in the preceding paper (Zoratti et al., 1985) and their simulations using the model in Figure 1 are within the conceptual framework of the classical delocalized protonic coupling (Mitchell, 1966). It has been suggested that the same kind of phenomenology would arise within the framework of a local intramembrane protonic coupling [coupling unit hypothesis, cf. Westerhoff et al. (1984)] if the resistance to proton back leakage within each coupling unit is relatively small compared to that between the local proton domain and the bulk phase (Westerhoff, 1983). However, within the framework of local energy coupling it appears difficult to account for the different behavior found with the two inhibitors antimycin and malonate [cf. Figure 7 in the preceding paper (Zoratti et al., 1985)]. Moreover, as a general observation, it is difficult to envisage a large disequilibrium between the local proton domains and the bulk aqueous phases at static head in the presence of oligomycin, the state in which the measurements were performed.

Registry No. H^+, 12408-02-5.

REFERENCES

Azzi, A., Casey, R. P., & Nalecz, M. J. (1984) *Biochim. Biophys. Acta 768*, 209–226.

Azzone, G. F., Zoratti, M., Petronilli, V., & Pietrobon, D. (1985) *J. Inorg. Biochem.* (in press).

Caplan, S. R. (1981) *Proc. Natl. Acad. Sci. U.S.A. 78*, 4314–4318.

Caplan, S. R. (1982) in *Dynamic Aspects of Biopolyelectrolytes and Biomembranes* (Oosawa, F., Ed.) pp 431–441, Kodansha, Tokyo.

Dancsházy, Zs., Groma, G. I., & Oesterhelt, D. (1984) *EBEC Rep. 3A*, 229–230.

Duszynsky, J., & Vojtczak, L. (1984) *EBEC Rep. 3A*, 233–234.

Frölich, O., Leibson, C., & Gunn, R. B. (1983) *J. Gen. Physiol. 81*, 127–152.

Gräber, P., Burmeister, M., & Hortsch, M. (1981) *FEBS Lett. 136*, 25–31.

Hill, T. L. (1977) *Free Energy Transduction in Biology*, Academic Press, New York.

Ho, Y., Jason Liu, C., Saunders, D. R., & Wang, J. H. (1979) *Biochim. Biophys. Acta 547*, 149–160.

Karlish, S. J. D., & Stein, W. D. (1982) *J. Physiol. 328*, 295–316.

Kedem, O., & Caplan, S. R. (1965) *Trans. Faraday Soc. 61*, 1897–1911.

Knauf, P. A., Fuhrmann, G. F., & Rothstein, A. (1977) *J. Gen. Physiol. 69*, 363–386.

Mitchell, P. (1966) *Chemiosmotic Coupling in Oxidative and Photosynthetic Phosphorylation*, Glynn Research Ltd., Bodmin, U.K.

Nicholls, D. (1974) *Eur. J. Biochem. 50*, 305–315.
Pentilla, T. (1983) *Eur. J. Biochem. 133*, 355–361.
Pick, U. (1984) *EBEC Rep. 3A*, 353–354.
Pietrobon, D., & Zoratti, M. (1982) *EBEC Rep. 2*, 255–256.
Pietrobon, D., & Caplan, S. R. (1985) *Biochemistry 24*, 5764–5776.
Pietrobon, D., Azzone, G. F., & Walz, D. (1981) *Eur. J. Biochem. 117*, 389–394.
Pietrobon, D., Zoratti, M., Azzone, G. F., Stucki, J. W., & Walz, D. (1982) *Eur. J. Biochem. 127*, 483–494.
Pietrobon, D., Zoratti, M., & Azzone, G. F. (1983) *Biochim. Biophys. Acta 723*, 317–321.
Portis, A. R., Jr., Magnusson, R. P., & McCarty, R. E. (1975) *Biochem. Biophys. Res. Commun. 64*, 877–884.
Ramirez, F., Okazaki, H., Tu, S.-I., & Hutchinson, H. (1983) *Arch. Biochem. Biophys. 222*, 464–472.
Schönfeld, M., & Neumann, J. (1977) *FEBS Lett. 73*, 51–54.
Serpersu, E. H., & Tsong, T. Y. (1984) *J. Biol. Chem. 259*, 7155–7162.
Sone, N., & Nicholls, P. (1984) *Biochemistry 23*, 6550–6554.
Soumarmon, A., Rangachari, P. K., & Lewin, M. J. M. (1984) *J. Biol. Chem. 259*, 11861–11867.
Tu, S.-I., Shiuan, D., Ramirez, F., & McKeever, B. (1981a) *Biochem. Biophys. Res. Commun. 99*, 584–590.
Tu, S.-I., Lam, E., Ramirez, F., & Marecek, F. (1981b) *Eur. J. Biochem. 113*, 391–396.
Walz, D. (1983) in *Biological Structure and Coupled Flows* (Oplatka, A., & Balaban, M., Eds.) pp 45–60, Academic Press, New York.
Westerhoff, H. V. (1983) Ph.D. Thesis, University of Amsterdam, Amsterdam, The Netherlands.
Westerhoff, H. V., & Dancsházy, Zs. (1984) *Trends Biochem. Sci. (Pers. Ed.) 9*, 112–117.
Westerhoff, H. V., Scholte, B. J., & Hellingwerf, K. J. (1979) *Biochim. Biophys. Acta 547*, 544–560.
Westerhoff, H. V., Melandri, B. A., Venturoli, G., Azzone, G. F., & Kell, D. B. (1984) *Biochim. Biophys. Acta 768*, 257–292.
Zoratti, M., Favaron, M., Pietrobon, D., & Azzone, G. F. (1986) *Biochemistry* (preceding paper in this issue).

Mucidin and Strobilurin A Are Identical and Inhibit Electron Transfer in the Cytochrome bc_1 Complex of the Mitochondrial Respiratory Chain at the Same Site as Myxothiazol†

Gebhard Von Jagow,‡ Gordon W. Gribble,§ and Bernard L. Trumpower*
Department of Biochemistry, Dartmouth Medical School, Hanover, New Hampshire 03756
Received July 15, 1985

ABSTRACT: Mucidin and strobilurin A, antifungal antibiotics isolated from the basidiomycetes *Oudemansiella mucida* and *Strobiluris tenacellus*, respectively, inhibit electron-transfer reactions in the cytochrome bc_1 complex of the mitochondrial respiratory chain. The two compounds have identical effects on oxidation–reduction reactions of the cytochromes *b* and c_1 in isolated succinate-cytochrome *c* reductase. They inhibit reduction of cytochrome c_1 by succinate but do not inhibit reduction of cytochrome *b*. When added in combination with antimycin, either inhibitor blocks reduction of both cytochromes *b* and c_1. Mucidin and strobilurin A differ from antimycin in that they inhibit, rather than promote, oxidant-induced reduction of cytochrome *b*. They also differ from antimycin in that they do not block reduction of cytochrome *b* by succinate when cytochrome c_1 is previously reduced by ascorbate and they do not inhibit oxidation of cytochrome *b* by fumarate. These effects of mucidin and strobilurin A are, however, qualitatively identical with those of myxothiazol, an antibiotic that inhibits respiration by binding to cytochrome *b* [Von Jagow, G., Ljungdahl, P. O., Graf, P., Ohnishi, T., & Trumpower, B. L. (1984) *J. Biol. Chem. 259*, 6319–6326]. Mucidin and strobilurin A have identical UV and mass spectra, and they elute together on high-pressure liquid chromatography. We thus conclude that these antibiotics, although isolated from different bacteria, are structurally identical. Our results indicate that strobilurin A and mucidin inhibit electron transport at the same site as myxothiazol and not at the antimycin site, as previously reported [Subik, J., Behren, M., & Musilek, V. (1974) *Biochem. Biophys. Res. Commun. 57*, 17–22].

Antibiotics that inhibit respiration provide an important approach for elucidating the pathway of electron transfer and mechanism of energy transduction in the cytochrome bc_1 complex of the mitochondrial respiratory chain. Thus, the effects of antimycin (Bowyer & Trumpower, 1981; De Vries et al., 1983) and myxothiazol (Meinhardt & Crofts, 1982; De Vries et al., 1983; Von Jagow et al., 1984) on oxidation–reduction reactions of the redox components of the bc_1 complex provide evidence that there are two pathways of cytochrome *b* reduction. This finding supports a protonmotive Q cycle pathway of electron transfer in the bc_1 complex (Mitchell, 1975, 1976; Bowyer & Trumpower, 1981; Meinhardt & Crofts, 1982; De Vries et al., 1983).

All antibiotic inhibitors of the bc_1 complex that have been characterized to date can be classified into one of two groups,

† This investigation was supported by NIH Grant GM 20379. B.L.T. is grateful to the Humboldt Stiftung for support provided by a Humboldt Preis.
‡ Present address: Institute of Physical Biochemistry, University of Munich, 8000 Munich 2, West Germany.
§ Present address: Department of Chemistry, Dartmouth College, Hanover, NH 03755.

0006-2960/86/0425-0775$01.50/0